

## General Disclaimer

metadata, citation and similar papers at [core.ac.uk](https://core.ac.uk)

brought to

provided by NASA Techn

One or more of the following statements may apply to this document.

- This document has been reproduced from the best copy furnished by the organizational source. It is being released in the interest of making available as much information as possible.
- This document may contain data, which exceeds the sheet parameters. It was furnished in this condition by the organizational source and is the best copy available.
- This document may contain tone-on-tone or color graphs, charts and/or pictures, which have been reproduced in black and white.
- This document is paginated as submitted by the original source.
- Portions of this document are not fully legible due to the historical nature of some of the material. However, it is the best reproduction available from the original submission.

(NASA-TM-85004) THE RELATIONSHIP BETWEEN  
SATURN KILOMETRIC RADIATION AND THE SOLAR  
WIND (NASA) 22 p HC A02/MF A01 CSCL 03B

N83-24445

Unclas  
11603

G3/90



Technical Memorandum 85004

# The Relationship Between Saturn Kilometric Radiation and the Solar Wind

M. D. Desch and H. O. Rucker

MARCH 1983

National Aeronautics and  
Space Administration

**Goddard Space Flight Center**  
Greenbelt, Maryland 20771



THE RELATIONSHIP BETWEEN  
SATURN KILOMETRIC RADIATION AND THE SOLAR WIND

M. D. Desch and H. O. Rucker<sup>1</sup>

Laboratory for Extraterrestrial Physics  
Planetary Magnetospheres Branch  
NASA/Goddard Space Flight Center  
Greenbelt, MD, 20771

Abstract. Voyager spacecraft radio, interplanetary plasma, and interplanetary magnetic field data are used to show that large amplitude fluctuations in the power generated by the Saturn kilometric radio emission are best correlated with solar wind ram pressure variations. In all, thirteen solar wind quantities previously found important in driving terrestrial magnetospheric substorms and other auroral processes were examined for evidence of correlations with the Saturn radio emission. The results are consistent with hydromagnetic wave or eddy diffusion processes driven by large scale solar wind pressure changes at Saturn's dayside magnetopause.

Introduction

Naturally occurring radio wave emission can serve as a remote diagnostic of physical conditions within distant magnetospheres. For example, long before in situ observations of the planets became possible, long-wavelength, groundbased measurements established the existence of Jupiter's magnetic field and the importance of Io as a body of astrophysical interest (see e.g., Carr et al. [1983]). In the case of Saturn, analysis of the radio emissions

<sup>1</sup> NAS/NRC Resident Research Associate, on leave from Institute for Space Research, Observatory, 8042 Graz, Austria.

has played a similar role. Observations of distinct storm episodes separated by about 10.6-hr, interpreted as a possible anomaly in the planet's near-surface magnetic field [Kaiser and Desch, 1982a], led to the first determination of Saturn's (magnetic) rotation period [Desch and Kaiser, 1981]. Inferences concerning Saturn's near-surface magnetic topology based on the radio astronomy observations have been especially provocative since the direct modeling of the main field indicates no longitudinally asymmetric features [e.g., Connerney et al., 1982] that might account for the 10.6-hr modulations. In the present paper we will further probe the magnetosphere of Saturn by studying the radio wave modulations that appear on a time scale of days rather than minutes or hours. We will show that the radio energy fluctuations that appear on these longer time scales are associated more directly with the ram pressure at Saturn than with any other plasma or magnetic solar wind property.

The first detections of Saturn's radio wave emissions were made from the Voyager 1 (V1) spacecraft by the Planetary Radio Astronomy (PRA) experiment. The observations showed that Saturn emits two distinctly different kinds of freely-propagating waves in the radio band: a relatively narrowband, polarized emission called Saturn Kilometric Radiation, or SKR [Kaiser et al., 1980], and a broadband, lightning-like emission called Saturn Electrostatic Discharge, or SED [Evans et al., 1981]. Both the SKR and SED sources radiate in excess of  $10^8$  watts into space and therefore are generated by significant non-thermal processes at Saturn. However, only the former is of interest in the present paper because of its value as a long-term remote sensor of magnetospheric conditions. Unlike the SED, whose source location has been in dispute (see e.g. Burns [1983] and Kaiser et al., [1983]) and which can only be observed within several days of spacecraft encounter with the planet, the SKR source location and beaming properties are relatively well known and the radiation is observable many months before encounter. These factors make the SKR an excellent monitor of the conditions for wave growth in the immediate vicinity of the radio source deep within Saturn's magnetosphere.

Several independent studies anticipated, to some degree, the existence of a direct solar wind interaction with Saturn's magnetosphere. For example, Kaiser and Desch [1982a] concluded from comparison of pre- and post-encounter observations that the SKR radio source must be confined to the high latitude, dayside auroral zone on Saturn. At this position near the dayside polar cusp,

a solar wind driven radio source seemed a likely possibility. Furthermore, during the Voyager 2 (V2) encounter with Saturn, a total disappearance of the SKR for about two days coincided with a possible immersion of Saturn in the extended tail or tail filament of Jupiter [Kurth et al., 1983]. A dropout in the SKR would be the expected response since the Saturn magnetosphere would have been shielded from direct solar wind interaction. Finally, Behannon et al., [1981] and Ness et al., [1982] attributed temporal variations in the structure of Saturn's magnetosphere to changes in solar wind conditions.

While each of these studies suggested a solar wind influence at Saturn, direct evidence was provided by Desch [1982] (hereafter paper 1) in a study of long-term SKR variations. Paper 1 established that the Saturn radio emission undergoes extreme fluctuations in radio energy on a time scale of days to weeks. It showed further that these variations depended strongly on solar wind conditions, specifically on ram pressure fluctuations. The principal long-term modulation period of the SKR was 25  $\pm$  2 days, coincident with the solar rotation period as viewed at Saturn. But while the evidence implicating ram pressure was fairly conclusive, paper 1 left open the question of exactly which solar wind property interacts most strongly with the magnetosphere to induce radio emission.

The present paper extends and improves on the analysis of paper 1 in several important ways in order to better define the nature of the solar wind interaction at Saturn. This has been accomplished (1) by defining an accurate quantitative measure of the radiated SKR wave energy, (2) by improving the time resolution over that used in paper 1 from 24-hr averages to 10.66-hr (one Saturn rotation) averages, and (3) by examining not only the solar wind plasma quantities but also various combinations of plasma and interplanetary magnetic field quantities and their correlation with the SKR.

### Solar Wind Quantities

Many solar wind parameters have been found important in stimulating magnetic substorms, auroral activity, and auroral kilometric radio emission (AKR) at the earth (see e.g. Akasofu [1981]; Gallagher and D'Angelo [1981]). In the present paper, we have examined the following: the solar wind bulk speed ( $V$ ) and  $BV^2$ , which correlate best with AKR [Gallagher and D'Angelo,

1981]; the interplanetary magnetic field (IMF) magnitude ( $B$ ); the solar wind ram pressure ( $P$ ), which was found in paper 1 to correlate well with SKR; the solar wind density ( $n$ ), which behaves very much like  $P$ ;  $\rho V^3$  and  $VB^2$ , which are associated with the kinetic and solar wind dynamo energy flux, respectively; the Akasofu parameter ( $\epsilon$ , see [Akasofu, [1981]]); the solar wind  $V^2 B_z$  (north and south), associated with the erosion of planetary field lines;  $B_y$  (toward and away from the sun), associated with magnetic sector boundary passages; and finally the magnitude of the solar wind electric field,  $|V \times B|$ . The  $z$  component of  $B$ , which is also used in calculating  $\epsilon$ , was cast in the coordinate system that contains Saturn's magnetic dipole axis and equatorial plane. The Akasofu parameter was redefined for Saturn by taking into account the fact that Saturn's magnetic axis is reversed relative to earth's.

#### Solar Wind and Radio Observations

We make use of data from three instruments on Voyager 1. Radio emission data are from the Planetary Radio Astronomy (PRA) experiment, interplanetary magnetic field data are from the Magnetometer (MAG) experiment, and solar wind plasma data are from the Plasma Science (PLS) experiment (see, respectively, Warwick et al., [1977]; Behannon et al., [1977]; and Bridge et al., [1977] for experiment descriptions).

An overview of the radio, plasma, and magnetic field quantities used in this paper is shown in Figure 1. The relative uncertainty in measuring these quantities is about 1% to 5% (see experiment descriptions), far less than the large-scale variations we will be concerned with in this paper. We have limited the analysis to V1 data for the  $\sim 6.7$  solar rotation interval from day 140 to 310, 1980. During this time the spacecraft moved from 1.6 AU (AU=astronomical unit) to within 0.1 AU of Saturn. Pre-encounter Voyager 2 data have not been used owing to the frequent encounter of the spacecraft with Jupiter's downstream magnetic tail, when no measurements of the solar wind are possible [Lepping et al., 1982]. Post-encounter SKR data are also not used because the combination of the nightside spacecraft departures and dayside radio source locations cause the emission to disappear as a result of small changes in source beam orientation [Kaiser and Desch, 1982b].

The top panel in Figure 1 shows the measured SKR radio energy per Saturn

rotation in units of joules/sr. The values shown were obtained by integrating the measured (1-hr averaged) SKR flux densities over the emission bandwidth (usually several hundred kHz) and integrating this spectral power over one Saturn rotation (10.66 hr). To avoid inverse-distance-squared bias, only those events were recorded, throughout the data set, that exceeded a flux density of  $3.5 \times 10^{-21}$  W/m<sup>2</sup>/Hz at 1 AU. This flux density represents an easily detectable signal level on day 140, the first day of the analysis interval. Linear interpolation across data gaps was used to complete each time history before final analysis. Linear interpolations were justified because none of the quantities change dramatically on interpolation-interval time scales. Data coverage was 90%, 86%, and 86% for the radio, plasma, and field data, respectively.

Over the duration of the period under study the SKR energy was seen to vary over a total range of more than two orders of magnitude, from a frequently observed minimum of about  $10^{11}$  joules/sr to over  $2 \times 10^{13}$  joules/sr on day 264. (In more familiar units, this corresponds to a range of isotropic power levels between about  $3 \times 10^7$  watts to  $7 \times 10^9$  watts.) By comparison, the minimum detectable energy level varied between about  $8 \times 10^{10}$  to  $8 \times 10^8$  joules/sr between days 140 and 310. The SKR was seen to remain at above average intensity for only a few rotations at a time; only rarely, at ~25-day intervals, did the output remain elevated for 10 rotations or more.

The second panel in Figure 1 shows the (Saturn) rotation-averaged solar wind ram pressure,  $P = \rho V^2$  in mks units of pascals, at Saturn over the same time interval as the SKR emission energy. This time series was generated in the following way: The pressure, measured at Voyager 1, was computed from 1-hr averaged density and bulk speed plasma data. The solar wind values were then ballistically projected to Saturn using a procedure in which the arrival time was determined from the known spacecraft-Saturn distance, the sun-Saturn-spacecraft angle, and the solar wind bulk speed. The maximum radial propagation delay was about 7 days and the maximum azimuthal delay was 0.2 days. Finally, running 10.66-hr averages were computed and the solar wind value was chosen that corresponded in time to that closest to the rotation phase of the SKR power cycle ( $90^\circ$  SLS) where the power is a maximum [Desch and Kaiser, 1981]. The reliability of extrapolating the solar wind to Saturn is discussed in a later section. Examination of Figure 1 shows that the pressure varied over several orders of magnitude, from about  $10^{-12}$  to over

$3 \times 10^{-10}$  pascals. The time scale of the variations was the same or slightly longer than the time scale of the SKR variations.

The third panel of Figure 1 shows the magnitude of the interplanetary magnetic field from day 140 to 310. The field data were handled in the same manner as the plasma data in deriving the averaged time series at Saturn. The field magnitude varied from less than 0.1 to 2.5 gamma over time scales comparable to that of both the pressure and radio energy.

### Correlation Results

Visual examination of Fig.1 shows a rather convincing overall correlation between the input quantities of ram pressure and magnetic field and the (presumed) output SKR time series. For example, major SKR episodes, centered on days 155, 182, 203, 228, 265, and 304, all coincide with similar enhancements in both ram pressure and magnetic field intensity. Furthermore, there are also striking correlations on shorter time scales apparent in these data: Figure 2 shows the interval from days 251 through 272 on an expanded scale. Here, the almost one-to-one correspondence between the SKR and ram pressure is evident; the correlation with magnetic field is less visually striking. Calculation of linear cross correlation coefficients bears this out: the correlation with pressure exceeds 80% at zero time lag (with respect to arrival time at Saturn) for this 22-day period, while the correlation with magnetic field is only 44%. Although this result applies only to a small subset of the data it suggests at the outset that ram pressure is a better predictor of SKR energy than magnetic field intensity alone.

Fig 1. shows in addition that there are also intervals of time during which neither quantity succeeds in matching the SKR profile, for example days 150, 199, 239-240, 299-301. On these days, no significant change is recorded in either the pressure or field magnitude values but the SKR is definitely enhanced. Thus, as was suggested in paper 1 and as is evident here, solar wind pressure is not by itself a perfect predictor of SKR energy. Several other combinations of solar wind plasma and field properties must be examined as alternatives.

The thirteen solar wind quantities described earlier were each examined for evidence of correlations with SKR. A time series of each of these parameters was generated in exactly the same way as was done for the pressure



and field magnitude data sets shown in Fig. 1. Linear cross correlations were computed between the SKR time series and each of the thirteen parameters. In order to make an unbiased estimate of the statistical significance of the correlations, each time series was also randomized to remove the tendency in all of the data sets for adjacent points in the same data set to be highly correlated (see e.g. Jenkins and Watts [1968], pp. 339-340). This procedure eliminates the artificially large correlations that can arise between two non-randomized time series. Further, with the data so randomized, the cross correlations can be expressed in terms of standard deviations, permitting unbiased statistical evaluation of the results.

Figure 3 (see also summary in Table 1) shows the results of cross correlating the SKR energy with each of the solar wind quantities over the 170-day analysis interval from day 140-310, 1980. The correlation coefficients are expressed in terms of the standard deviation ( $\sigma$ ) as a function of time from about -26 days to +26 days correlation lag, or about +1 solar rotation. The convention used here has positive time lag corresponding to physically realizable correlations in that SKR energy changes follow in time the corresponding changes in the solar wind value. Negative lag times violate causality. Table 1, in which the values of the peak correlation coefficients and the time lag of the peaks are listed for easy reference, also includes results for the correlation of SKR with solar wind density,  $\rho$ .

The superiority of the solar wind pressure (P) and kinetic energy flux ( $\rho V^3$ ) as predictors of radio energy is clear. The peak correlations with both parameters occur at zero time lag (+10.66 hrs) with a magnitude of nearly  $6\sigma$  above the mean. The density (see Table 1) also shows a highly significant correlation with SKR. It should be noted that P and  $\rho V^3$  are dominated largely by variations in  $\rho$ . The time histories of these three quantities are nearly indistinguishable from one another in spite of multiplication by factors up to  $V^3$ . It is therefore not surprising that  $\rho$ , P, and  $\rho V^3$  all show similar degrees of correlation with SKR. We have examined more closely the effect of the speed on the results by correlating SKR with the term  $\rho V^n$ , where n is allowed to vary between 0 and 3. The peak correlation occurs with n between 2.4 and 2.5, but the variation in the computed correlations is not very large. We will thus consider that the pressure,  $\rho V^2$ , is the best predictor of SKR, significantly better than density alone. The kinetic energy flux,  $\rho V^3$ , and  $\epsilon$  will be discussed separately below, in the context of the solar wind

energetics at Saturn.

The next best correlation is with solar wind speed, which is  $4.2\sigma$  above the mean. Except for the quantities  $\rho V^3$  and  $\epsilon$ , all other quantities have peaks less than or equal to about  $3\sigma$  for delay times within  $\pm 1$  Saturn rotation about zero time lag. Non-randomized linear cross correlation coefficients varied from 36% to only 14% for all quantities other than pressure and  $\rho V^3$ , which peaked at 52% and 49%, respectively. Note that some of the correlations shown in Figure 3 have a tendency to exhibit secondary peaks at lag times of about  $\pm 60$  rotations ( $\pm 26$  days). This is due to the  $\sim 26$ -day solar-rotation periodicity present in nearly all of the data sets.

The fact that some of the quantities, namely B,  $B_y$  (away), V, and  $BV^2$  reach or exceed  $3\sigma$  for reasonable (i.e.  $\pm 1$  Saturn rotation) time delays might suggest that these quantities are also effective in stimulating SKR. For several reasons this is probably not the case. First, it is well known that the solar wind quantities examined here are all correlated with each other to some degree. Figures 1 and 2, for example, show a close dependence between pressure (essentially density) and B, with the signatures tracking each other reasonably well. In fact, the magnitude of the correlation between B and P for the period from day 140 to 310 is over 81%. Any quantity that is correlated with pressure will also exhibit a degree of correlation with SKR. Therefore the relatively small correlation coefficients between SKR and all quantities other than pressure suggest strongly that these correlations are due solely to their inherent relationship with pressure.

To explore this point further, we examined the effect on the results of cross correlating only one-half of the data set to see which properties persisted in showing relatively high ( $>3\sigma$ ) correlations. The interval examined extended from days 215-310, 1980, approximately the second half of the previous analysis interval. The radial and azimuthal solar wind propagation times to Saturn were a maximum of  $\sim 3.5$  days and 0.1 days, or about one-half of the maximum for the full data set. Thus this procedure also addresses the issue of what effect possible problems with propagating the solar wind to Saturn might have on the correlations. The results, shown in Table 1, again showed that  $\rho$ , P, and  $\rho V^3$  correlated best with SKR, although the correlation with  $\rho$  was significantly less than that with P or  $\rho V^3$ . The linear correlation coefficient with pressure was 71%. The other quantities remained about the same or decreased. Note that the correlation with V

dropped to  $2.7\sigma$ , for example. These results support the contention that only terms involving  $pV^n$  are significant in stimulating SKR. All other examined quantities exhibit relatively small and variable correlations, due only to their intercorrelations with pressure. Based on the results for the complete 170-day data set, we conclude that the pressure is the most important quantity in the stimulation of SKR.

Because the z component of the interplanetary magnetic field is so important in geomagnetic interactions, we examined the Bz-SKR correlations with particular interest (see Figure 3 and Table 1). The correlations were done in the standard way. For the correlation with Bs (south) we set

$$\begin{aligned} B_s &= -B_z \quad (B_z < 0) \\ B_s &= 0 \quad (B_z > 0); \end{aligned}$$

and for Bn,

$$\begin{aligned} B_n &= B_z \quad (B_z > 0) \\ B_n &= 0 \quad (B_z < 0). \end{aligned}$$

The quantities Bs, VBs,  $V^2Bs$ , and the equivalent northern-directed quantities were all studied, but only the results for  $V^2Bs$  and  $V^2Bn$  are shown. In Figure 3 there is certainly a suggestion that  $V^2Bn$  performs better than  $V^2Bs$  in predicting SKR, although the magnitude of the correlations is only  $2.8\sigma$  and  $1.0\sigma$ , respectively, for physically reasonable ( $\pm 1$  rotation) lag times. A correlation with Bn might be the expected behavior in the case of a magnetosphere like Saturn's whose axis is reversed relative to the earth's. That is, northern excursions of the IMF might be expected to erode the dayside planetary field since the field lines emanate from the northern saturnigraphic pole and are directed toward the  $-z$  direction at the equator. We do not believe this result has much credibility, however, because when the analysis interval is shortened to days 215-310, 1980, the tendency for Bn to be preferred over Bs disappears and both correlations are less than  $1.2\sigma$  at zero lag. The peak correlations for Bn and Bs, which were at lags of  $-3$  and  $-4$  rotations, were only  $1.9$  and  $2.9\sigma$ , respectively. Not only is there no significant correlation with SKR, but the peaks occur at non-physical lag times and there is no significant difference seen between Bn and Bs. Further,

ORIGINAL PAGE IS  
OF POOR QUALITY

the results for the quantities VBz and Bz were not noticeably different from those for  $V^2Bz$ . We conclude that there is no evidence that the north-south component of the field influences SKR enhancements.

### Solar Wind Propagation

Implicit in the analysis so far has been the assumption that the solar wind was successfully projected from its measurement point at Voyager 1 to the interaction point at Saturn. The propagation times varied over a wide range, from about 7 days, on day 140, to only several hours, on day 310. Throughout the interval, however, the propagation between V1 and Saturn was almost purely radial because the sun-centered angular separation between Voyager 1 and Saturn never exceeded  $3.2^\circ$ . Thus there was never more than about 0.2 days of angular propagation delay to account for. As mentioned, we used simple ballistic propagation, which does not take interacting high and low speed streams into account, although a time reordering of the data was performed to account for high speed plasma streams arriving ahead of low speed plasma.

In order to assess the level of uncertainty inherent in the V1-to-Saturn propagations, we compared solar wind observations made by Voyagers 1 and 2 from Jan 5, 1978 through March 2, 1979, that is, up to the time of V1 encounter with Jupiter on March 5. During this time the V1-V2 spacecraft separation increased from about zero distance to almost 0.6 AU, or approximately 0 to almost 2 days solar wind propagation delay. The sun-centered V1-V2 angular separation increased to over  $3.5^\circ$ , slightly more than the maximum V1-Saturn separation geometry. Thus the V1-V2 radial separation was less than the maximum V1-Saturn separation, but the angular separation range was greater.

The measured solar wind quantities of density, speed, B, Bz, and VxB were used in testing the procedure for propagating solar wind characteristics between V1 and V2. Ten-hour running averages were used and successive 30 to 45 day spans of data were correlated over the 14-month analysis interval. The solar wind speed showed the highest correlation, consistently near 95%. Density and B showed correlations in the range 80-90% and 85-90%, respectively. The correlations between Bz values at the two spacecraft were the lowest, varying between about 45% and 66%. Thus the magnitudes of the

generally high degree of correlation was probably due to the long averaging interval used (10 hr), chosen to match closely that used in the solar wind-SKR correlations. With 10-hour resolution, the solar wind at the downstream spacecraft could be predicted reliably.

Although the V1-V2 test of Bz correlations did not yield values as large as those of density, speed, and B, we believe the conclusions drawn previously, namely that Bz shows no significant association with SKR, are justified. Note in Table 1 that the peak Bz-SKR correlations tend to occur at lags well outside the acceptable  $\pm 1$  rotation limit, yet we succeeded in predicting the arrival times to within  $\pm 10$  hours in the V1-V2 study (see below). Furthermore, no significant improvement was noted in the correlation between SKR and Bz in the shortened analysis interval (days 215-310) in which solar wind propagation effects are at a minimum.

We conclude that the high correlation between SKR and pressure can not be attributed simply to a higher level of confidence in propagating solar wind density to Saturn. The V1-V2 correlation with speed was higher than that for density but speed showed a much less significant correlation with SKR than did pressure in the long analysis interval, and no correlation in the short interval (see Table 1). Also, B and Bz are both reasonably well predicted downstream, yet they also show no significant correlation with SKR. Thus there is no apparent relationship between the degree of confidence with which individual solar wind quantities were propagated between V1 and V2 and the degree of correlation of those quantities with SKR.

This conclusion is supported by the analysis of data taken when V1 was very close to Saturn (day 215-310), that is when the propagation effects were at a minimum. These results (Table 1) continued to show an overwhelming preference for a pressure-related dependence and no significant dependence on any other quantity.

We examined with particular attention the arrival times of features at the downstream spacecraft. We found that the observed arrival times varied by up to  $\pm 10$  hours from those predicted. Thus a valid question that arises from the V1-V2 comparison is what effect an uncertainty in arrival time has on the measured cross correlations with SKR. The departures from predicted arrival times were equal to about one averaging interval in the SKR correlation analysis. Applying this uncertainty to the SKR correlation results, we determined the decrease in the correlation between SKR and pressure by adding

a random number, between  $\pm 10.66$  hrs, to the total transit times between V1 and Saturn. The effect on the correlation coefficient was not large; the correlation between SKR and pressure decreased by only one part in six. Similar small changes in the correlation coefficients were observed for other solar wind quantities, none large enough to cause concern about the V1 to Saturn projections nor to materially affect the conclusions we have drawn so far.

### Energetics

It is apparent that the dominant energy source ultimately responsible for the stimulation of SKR appears in the form of solar wind ram pressure variations, and that quantities involving IMF magnitude and direction are relatively unimportant. Comparison of the quantities  $\rho V^3$  and  $\epsilon$ , which characterize the solar wind kinetic energy flux and solar wind dynamo energy flux, respectively [Akasofu, 1981], provides a good way to summarize and reinforce this conclusion. Additionally, with the SKR expressed in terms of its isotropic energy flux (watts), the absolute power levels involved in the solar wind input and radio wave output terms are explicit. Figure 4 shows the SKR, kinetic, and dynamo power levels for days 215 to 310. To express the solar wind quantities in terms of watts, they have been multiplied by  $(20 R_s)^2$ , where  $20 R_s$  ( $R_s=60330$  km) is the magnetopause standoff distance, a good measure of the magnetosphere cross section (see e.g., Figure 1 of Behannon et al. [1981]). The magnitude of the cross correlation with SKR at zero time lag is shown in parentheses for each solar wind quantity. The correlation of  $\rho V^3$  with SKR peaked at zero time lag with a value of 73%. The correlation of  $\epsilon$  with SKR peaked at a lag of -2 rotations with a relatively small value of 44% (34% at zero time lag). Thus the correlation with  $\epsilon$  is non-physical since it indicates SKR fluctuations are preceding changes in  $\epsilon$  on the average. However, the correlation with  $\rho V^3$  is substantial at  $5\sigma$  above background and the peak occurs at a physically meaningful time lag. Therefore with the input and output terms expressed in identical units, it is apparent that the kinetic energy flux, which contains the ram pressure, predicts SKR intensities far better than does the term that takes both IMF magnitude and direction into account.

Note also that the power emitted by the radio waves is only a small

fraction of either the kinetic or dynamo flux incident on Saturn's magnetosphere. This statement is also true in the case of the Jovian emission and the terrestrial radio emission, both of which represent only small fractions of the total solar wind energy incident onto their respective magnetospheres. Although several stages may be needed to couple energy from the solar wind into the radio generation region, the efficiency of each step need not be large. The overall efficiency for the conversion into SKR energy of the kinetic energy flux contained in the solar wind is between  $10^{-4}$  and  $10^{-5}$ .

#### Summary and Discussion

The primary driver of the long-term fluctuations in Saturn's radio energy output is the solar wind ram pressure. The association of SKR with other non-pressure-related solar wind quantities is not significant and probably is no greater than would be expected on the basis of the known intercorrelations of these quantities with the ram pressure. The pressure correlation peak occurs at zero time lag, consistent with a time delay of less than 1 Saturn rotation between the onset of a ram pressure increase and the beginning of an increase in SKR energy. Assuming a magnetosphere cross sectional radius of 20  $R_s$  exposed to the solar wind, the SKR radio power represents between .01% and 0.001% of the kinetic energy flux incident on Saturn's magnetosphere.

We mentioned at the outset, based on examination of Figure 1, that the pressure was not a perfect predictor of SKR energy. We now know in addition that no other solar wind quantity offers an improvement. There are several possible reasons for the imperfect correlation between SKR and pressure. First, we have not accounted for the evolution of the solar wind flow as it propagates from the spacecraft to Saturn. The interactions that take place as high-speed streams overtake low-speed plasma might alter the pressure profile enough to account for the 'missing' and difficult to explain SKR peaks. However, a full MHD analysis of the solar wind flow would be required to take the interactions into account and this is beyond the intended scope of this paper. Another source of uncertainty is considered the more likely origin of the imperfect correlation. This concerns the unknown series of interactions between the arrival of a given solar wind stream at Saturn and the emission of SKR. The observed efficiency of this process is less than

ORIGINAL MANUSCRIPT  
OF POOR QUALITY

0.01%, so that certainly several inefficient steps are involved in the energy transfer, about which nothing quantitative is known. In view of this, the degree of correlation with pressure that is observed, reaching 71% for the short analysis interval, is singularly large. By comparison, the peak correlation coefficient between the earth's AKR and the solar wind speed was observed to be only 78% [Gallagher and D'Angelo, 1981], and virtually no uncertainties due to solar wind projections were present in the AKR study. We conclude that the less-than-perfect association between SKR and solar wind pressure is due to the poorly-understood nature of the processes that take place between the initial and final stages of the conversion from solar wind particle energy to electromagnetic energy.

Arguing by analogy with the way in which the solar wind interacts with the earth's magnetosphere, we can speculate as to the nature of the intermediate steps between solar wind arrival at Saturn and emission of SKR. Based on what is known about the terrestrial case, we might have expected the SKR to correlate best with IMF direction or some quantity associated with it, like  $\epsilon$ . The fact that we find no evidence for such an association is not to say, of course, that Saturn's magnetosphere does not respond, and even respond dramatically, to IMF variations. All we can say for certain is that the radio emission process is not sensitive to such quantities. This may not be surprising in view of the fact that the terrestrial kilometric radiation intensity also does not respond appreciably to IMF-associated quantities, but correlates best with solar wind speed [Gallagher and D'Angelo, 1981]. While the exact situation with regard to all of the various Jovian emissions is unclear [Carr et al., 1983], it may be true in general that the planetary radio emissions do not respond directly to the IMF.

In view of this, we must look to a mechanism whereby kinetic pressure variations can induce changes in radio energy at Saturn. We know that the SKR radio source is located on field lines that map down along Saturn's dayside polar cusps [Kaiser and Desch, 1982a] with the source altitude at any given radio frequency ( $f$ ) probably given by the place where  $f = f_g$  ( $f_g$  = electron gyrofrequency). This would place the source within the range of about .05 to 3  $R_s$  from Saturn's cloud tops, essentially what might be called the low altitude dayside cusp. With the radio source so situated, field aligned currents associated with the dayside polar cap boundaries are likely to be the direct drivers of plasma instabilities leading to wave growth and radio



ORIGINAL PAGES  
OF POOR QUALITY

emission. In support of this idea we note that in the terrestrial case a direct correlation has been observed between the occurrence of the auroral kilometric radiation and auroral field-aligned currents [Green et al., 1982].

Suggestions as to how these currents might in turn be driven by solar wind-magnetosphere interactions come from several studies. We are primarily interested in non-IMF related interactions, and since IMF-magnetosphere interactions are most easily understood in terms of the open-magnetosphere concept, we have looked toward energy transfer schemes that at least a priori do not require open magnetospheres.

One such approach involves the generation of low-frequency hydromagnetic (HM) waves in the magnetosheath/boundary layer region, either by solar wind pressure variations or Kelvin-Helmholtz (KH) instabilities. Small amplitude surface waves on Saturn's magnetopause, probably caused by KH instabilities, have in fact been observed with Voyager 1 [Lepping et al., 1981]. In the case of the earth, Eastman et al. [1976] have shown that this boundary layer, or entry layer, acts like an MHD generator, converting the kinetic energy of moving plasma to the electrical energy contained in field-aligned currents. As such, it is the site of continuous plasma, momentum, and energy transfer from the magnetosheath to the magnetosphere. The mechanism is at least indirectly responsible for, among other things, the field aligned currents that border the earth's dayside polar caps. Whether or not these currents respond directly to external pressure variations at Saturn is still an open question since there is no direct evidence, even at earth, that magnetosheath activity induces radio fluctuations. However, it is quite possibly a plausible scenario for stimulating SKR.

The mechanism for solar wind energy transport proposed by Eastman et al. [1976] involves diffusion of particles into the magnetosphere. A more direct and possibly faster interaction scheme has been observed at earth by Haerendel et al. [1978], and involves the continuous mass transfer of particles from the solar wind into the low altitude cusps. The mechanism proceeds by means of eddy convection in the dayside polar cusp/magnetosheath region. Haerendel et al. have shown that this entry layer in the cusp shows no particular dependence on the IMF z component. The magnetopause boundary in this region is, however, in constant motion due to pressure fluctuations, although the time scale on which these motions have been measured is only tens of seconds, much shorter than might be of interest in the present

context. As inferred from the results presented here, we would require an increase in the eddy diffusion coefficient in Saturn's dayside polar cusp region as a consequence of large scale pressure enhancements occurring on a time scale of hours to days. This would increase plasma transfer through the entry layer and into the low altitude cusp where the SKR power is amplified.

The scheme proposed here to couple solar wind energy to the radio generation site via pressure fluctuations and HM waves or convection in the cusps is largely conjectural. This is due to the fact that the necessary in situ observations of Saturn's magnetosphere have been limited to three brief spacecraft encounters, and even in the case of the earth, details of similar energy coupling mechanisms are not completely understood. For Saturn, the most remotely sampled magnetosphere yet visited, it is hoped that more intensive analysis of radio, plasma, and magnetic field data from the Voyager spacecraft will shed some light on this problem.

Acknowledgments. We are especially grateful to N. F. Ness, Voyager Magnetometer team principal investigator, and to H. S. Bridge, Plasma Science team principal investigator, for making the necessary data available for this study. We have also benefitted greatly from discussions with J. K. Alexander, L. F. Burlaga, R. P. Lepping, N. F. Ness, J. E. P. Connerney, J. H. King, K. H. Behannon, and M. L. Kaiser.

#### References

Akasofu, S. -I., Energy coupling between the solar wind and the magnetosphere, Space Sci. Rev., 28, 121, 1981.

Behannon, K. W., et al., Magnetic field experiment for Voyagers 1 and 2, Space Sci. Rev., 21, 235, 1977.

Behannon, K. W., J. E. P. Connerney, and N. F. Ness, Saturn's magnetic tail: structure and dynamics, Nature, 292, 753, 1981.

Bridge, H. S., et al., The plasma experiment on the 1977 Voyager mission, Space Sci. Rev., 21, 259, 1977.

Burns, J. A., M. R. Showalter, J. N. Cuzzi, and R. H. Durisen, Saturn's electrostatic discharges: could lightning be the cause?, Icarus, 1983, in press.

Carr, T. D., M. D. Desch, and J. K. Alexander, Phenomenology of magnetospheric radio emissions, Physics of the Jovian Magnetosphere, edited by A. J. Dessler, Cambridge University Press, 1983.

Connerney, J. E. P., M. H. Acuna, and N. F. Ness, Zonal harmonic model of Saturn's magnetic field from Voyager 1 and 2 observations, Nature, 298, 44, 1982.

Desch, M. D., Evidence for solar wind control of Saturn radio emission, J. Geophys. Res., 87, 4549, 1982.

Desch, M. D., and M. L. Kaiser, Voyager measurement of the rotation period of Saturn's magnetic field, Geophys. Res. Lett., 8, 253, 1981.

Eastman, T. E., E. W. Hones, Jr., S. J. Bame, and J. R. Asbridge, The magnetospheric boundary layer: site of plasma, momentum and energy transfer from the magnetosheath into the magnetosphere, Geophys. Res. Lett., 3, 685, 1976.

Evans, D. R., J. W. Warwick, J. B. Pearce, T. D. Carr, and J. J. Schauble, Impulsive radio discharges near Saturn, Nature, 292, 716, 1981.

Gallagher, D. L., and N. D'Angelo, Correlations between solar wind parameters and auroral kilometric radiation intensity, Geophys. Res. Lett., 8, 1087, 1981.

Green, J. L., N. A. Saflekos, D. A. Gurnett, and T. A. Potemra, A correlation between auroral kilometric radiation and field-aligned currents, J. Geophys. Res., 87, 10463, 1982.

Haerendel, G., et al., The frontside boundary layer of the magnetosphere, J. Geophys. Res., 83, 3195, 1978.

Jenkins, G. M., and D. G. Watts, Spectral Analysis and its Applications, Holden-Day, San Francisco, 1968.

Kaiser, M. L., and M. D. Desch, Saturnian kilometric radiation: source locations, J. Geophys. Res., 87, 4555, 1982a.

Kaiser, M. L., and M. D. Desch, Beaming properties of saturnian kilometric radiation, EOS, 63, 1068, (abstract), 1982b.

Kaiser, M. L., J. E. P. Connerney, and M. D. Desch, The source of Saturn electrostatic discharges: atmospheric storms, Nature, 1983, in press.

Kaiser, M. L., M. D. Desch, J. W. Warwick, and J. B. Pearce, Voyager detection of nonthermal radio emission from Saturn, Science, 209, 1238, 1980.

Kurth, W. S., J. D. Sullivan, D. A. Gurnett, F. L. Scarf, H. S. Bridge, and E. C. Sittler, Jr., Observations of Jupiter's distant magnetotail and wake, J. Geophys. Res., 87, 10373, 1983.

Lepping, R. P., L. F. Burlaga, M. D. Desch, and L. W. Klein, Evidence for a distant (>8700 R<sub>J</sub>) Jovian magnetotail, Geophys. Res. Lett., 9, 885, 1982.

Lepping, R. P., L. F. Burlaga, and L. W. Klein, Surface waves on Saturn's magnetopause, Nature, 292, 750, 1981.

Ness, N. F., et al., Magnetic field studies by Voyager 2: preliminary results at Saturn, Science, 215, 558, 1982.

Warwick, J. W., J. B. Pearce, R. G. Peltzer, and A. C. Riddle, Planetary radio astronomy experiment for Voyager missions, Space Sci. Rev., 21, 309, 1977.

ORIGINAL PAGE IS  
OF POOR QUALITY

TABLE 1. Peak Correlations and Lag Times

Solar	<u>80140 - 80310</u>		<u>80215 - 80310</u>	
Wind				
Property	$\sigma$	Lag	$\sigma$	Lag
$\rho$	5.5	0	4.7	0
P	5.9	0	4.9	0
$\rho V^3$	5.9	0	5.0	0
B	3.0	-1	2.4	0
V	4.2	0	2.7	+1
$\epsilon$	3.6	-1	3.1	-3
$VB^2$	2.6	-1	2.7	-2
$BV^2$	3.2	0	2.7	+1
$V^2_{Bn}$	2.8	-1	1.9	-3
$V^2_{Bs}$	2.9	-3	2.9	-4
$B_y(t)$	3.7	-2	2.6	-1
$B_y(a)$	3.3	+1	3.2	0
$ V \times B $	3.5	-2	2.3	-2

Lag in units of Saturn rotations  
Negative lags violate causality

## Figure Captions

Fig. 1. Survey plot of Voyager 1 Planetary Radio Astronomy, Plasma Science, and Magnetometer data for the 170-day interval from day 140 to 310, 1980. The Saturn kilometric radiation (SKR) energy per rotation (joules/sr) is compared with the solar wind ram pressure and interplanetary magnetic field (IMF) magnitude at Saturn.

Fig. 2. Expanded plot of data shown in Figure 1 showing near one-to-one correlation between ram pressure and SKR energy. Data are for the interval from day 251 through 272, 1980.

Fig. 3. Correlations in terms of  $\sigma$  between the SKR energy and twelve solar wind quantities for the interval from day 140 to 310, 1980. The ram pressure,  $P$ , and the closely related quantity  $\rho V^3$  show the highest correlation.

Fig. 4. Survey plot of the SKR power and solar wind kinetic power ( $\rho V^3$ ) and magnetic dynamo power ( $\epsilon$ , the Akasofu parameter) for the period from day 215 to 310, 1980. The linear correlation coefficient of each parameter with the SKR at zero days lag is shown in parenthesis.

ORIGINAL PAGE IS  
OF POOR QUALITY

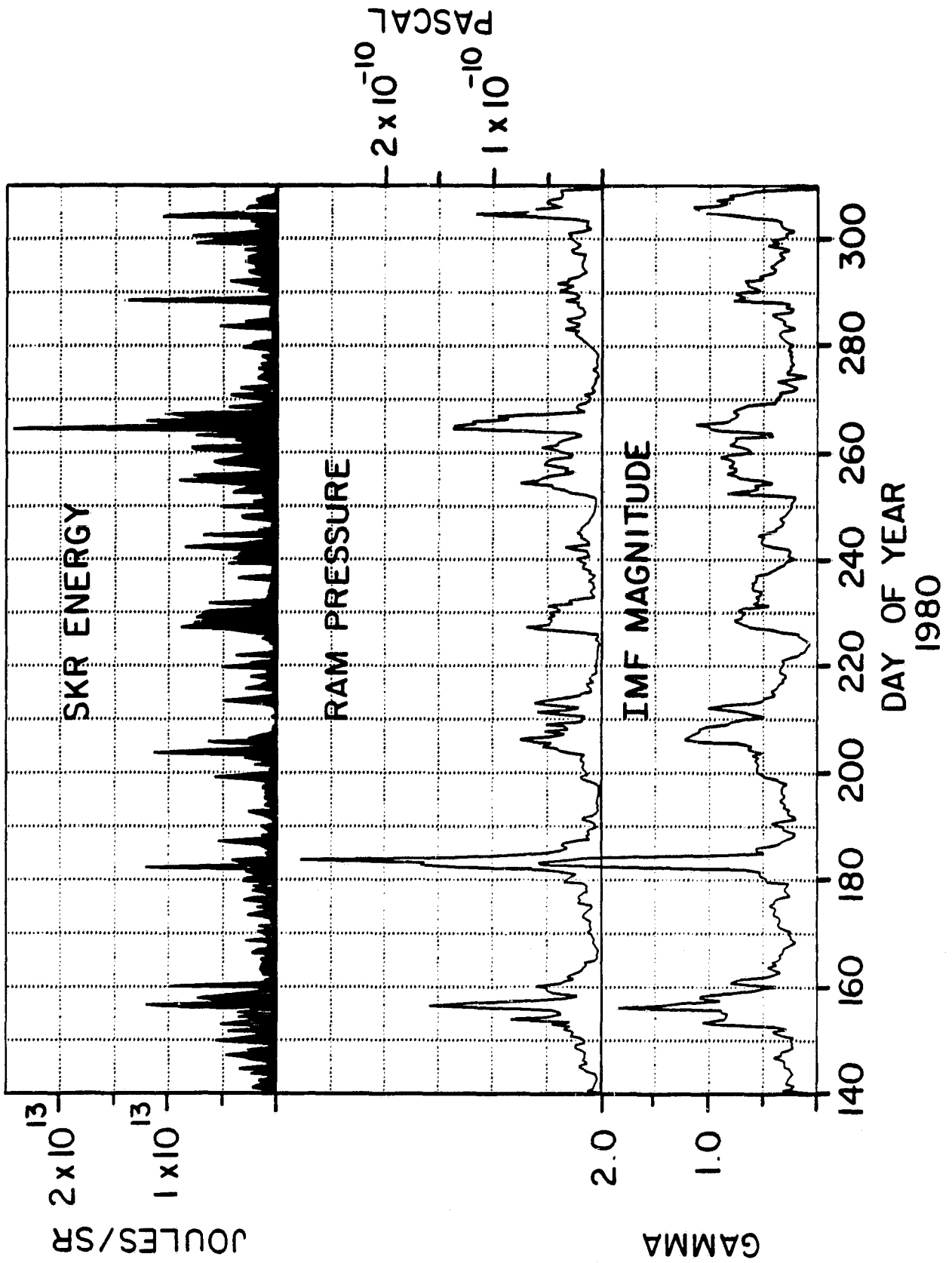


Figure 1

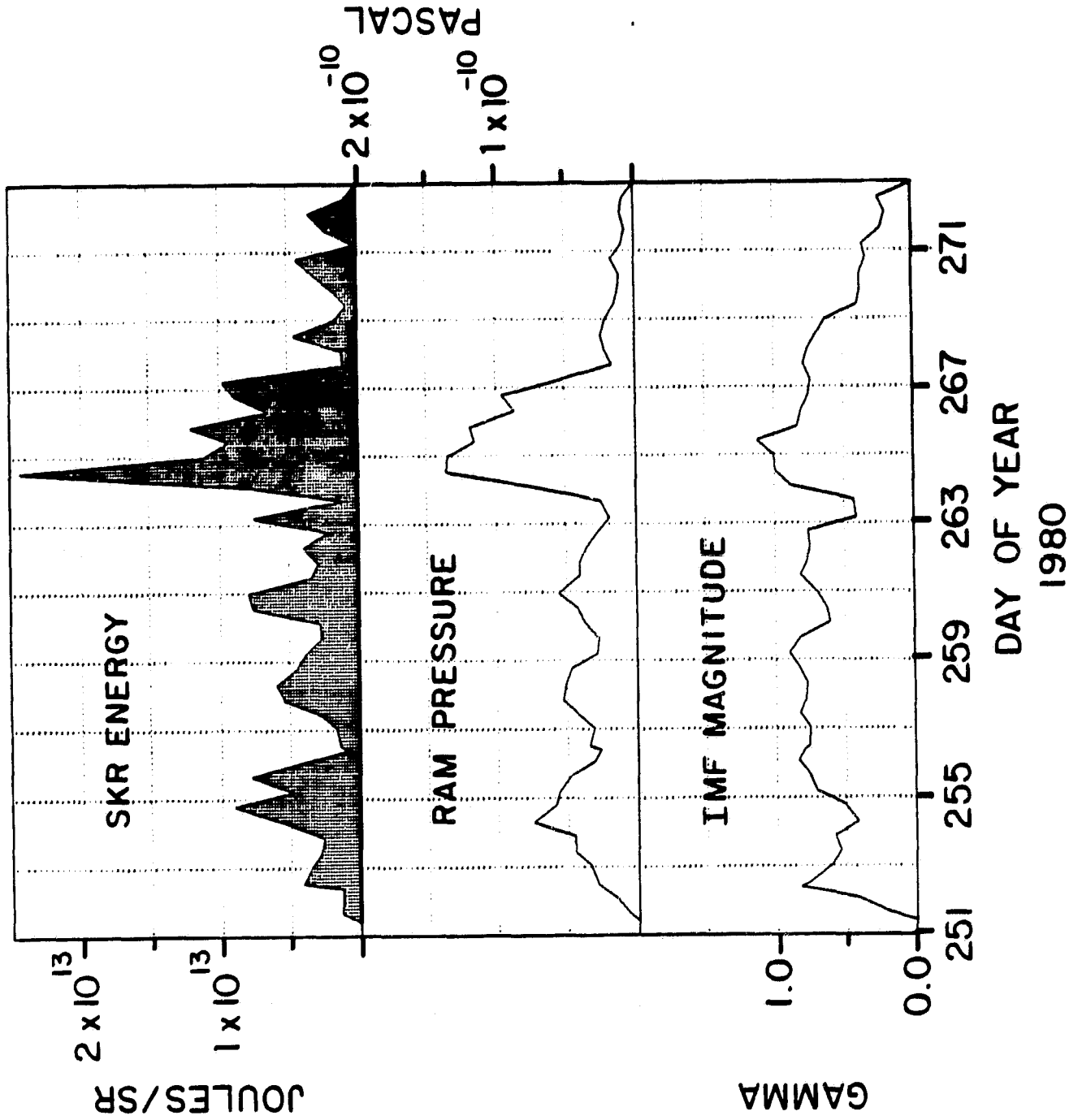


Figure 2



ORIGINAL FIGURE  
OF POOR QUALITY

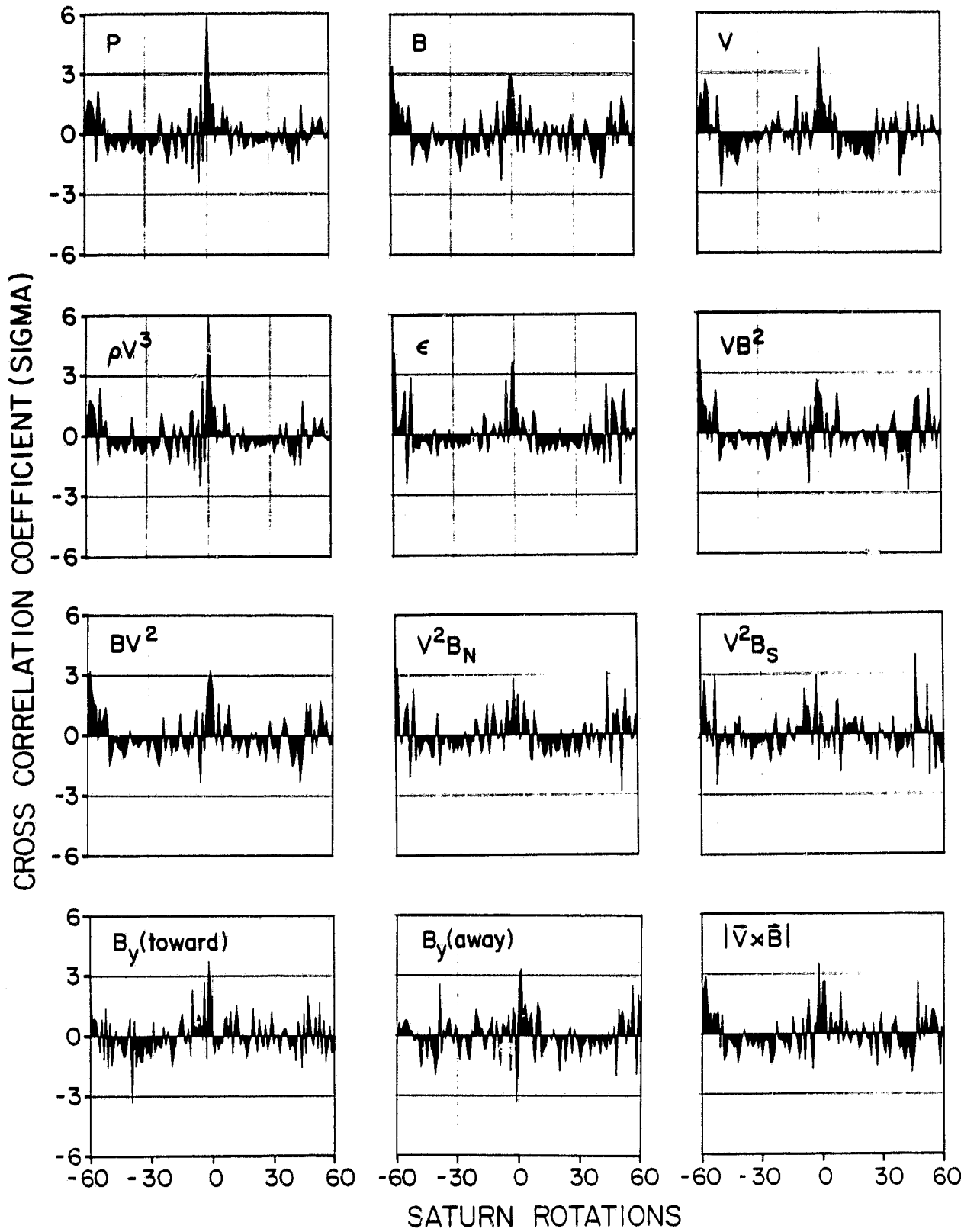


Figure 3

ORIGINAL FIGURE  
OF POOR QUALITY

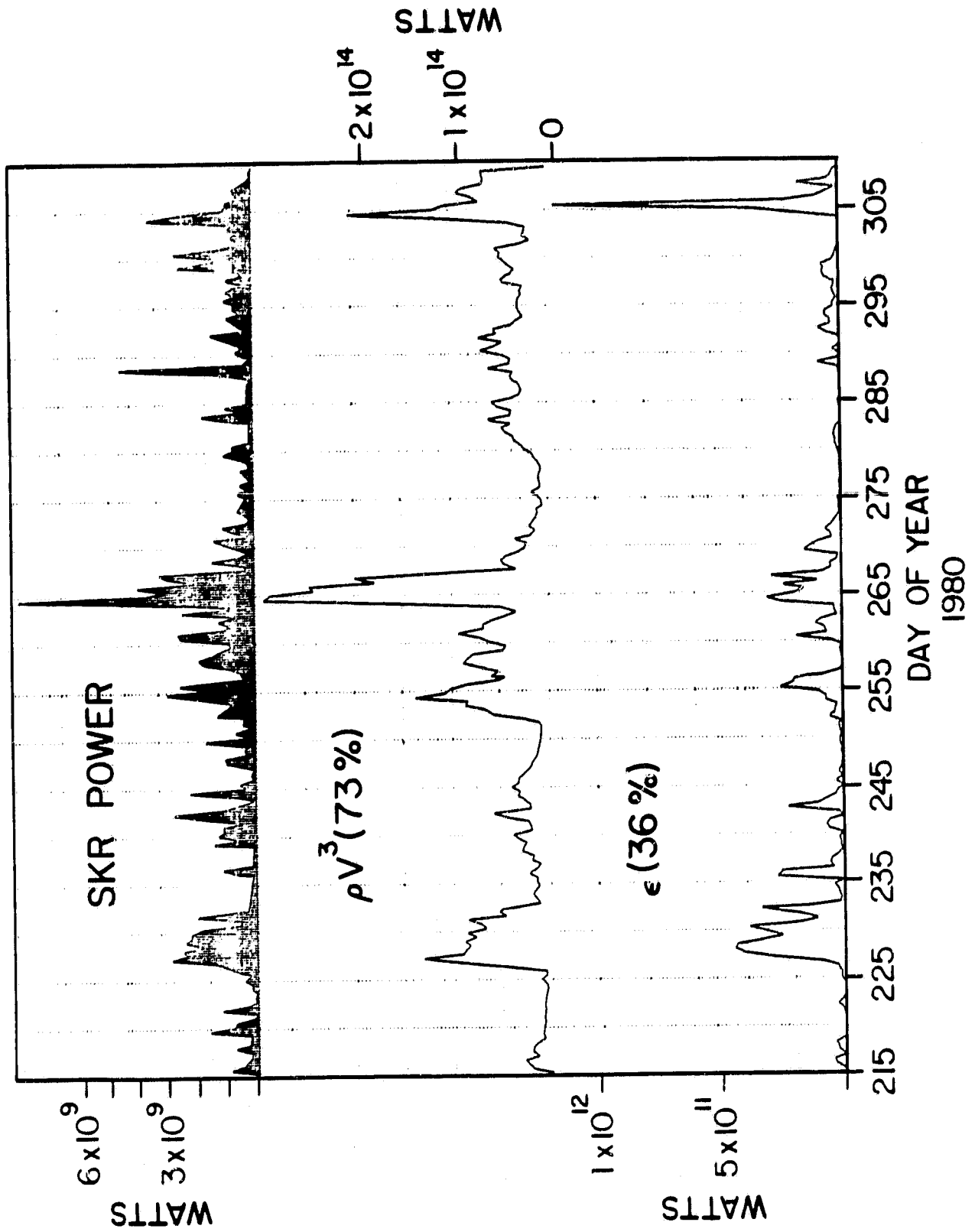


Figure 4